International Journal of Environmental Sciences
ISSN: 2229-7359
Vol. 11 No. 23s,2025
https://theaspd.com/index.php

Structural, Morphological, And Electrical Properties Of Zinc-Doped Silver Oxide Thin Films Synthesized By Spray Pyrolysis Method

Deepak Kumar[1], Vikram Singh[2*]
[1,2]Department of Physics, OSGU, Hisar
EMAIL: d.k.ghorela@gmail.com[1], vikramdobal@gmail.com*[2]

Abstract
This study investigates the synthesis, characterization, and electrical properties of zinc-doped silver oxide (Ag_2O) thin films produced via the spray pyrolysis method. The films were synthesized with varying zinc doping concentrations (1%, 3%, and 5%) and characterized using Fourier Transform Infrared Spectroscopy (FTIR), X-ray Diffraction (XRD), Scanning Electron Microscopy (SEM), and Transmission Electron Microscopy (TEM). FTIR and XRD analyses confirmed the successful formation of silver oxide and revealed changes in the crystallinity and phase composition with increasing zinc doping. SEM and TEM images demonstrated that zinc doping led to an increase in grain size and improved film uniformity. DC conductivity measurements showed a significant increase in conductivity with higher zinc doping concentrations, with the highest conductivity observed at 5% doping. The temperature dependence of conductivity followed an Arrhenius behavior, with reduced activation energy at higher zinc concentrations. This study highlights the potential of zinc-doped silver oxide thin films for applications in electronics, sensors, and transparent conductive coatings.
Keywords: *Conductivity, FTIR, Spray pyrolysis, Thin films, XRD, Zinc-doped silver oxide*

1. INTRODUCTION

Thin films of metal oxides, particularly silver oxide (Ag_2O), have garnered significant attention in recent years due to their wide range of applications in electronics, optoelectronics, and energy storage devices. Silver oxide thin films are valued for their semiconducting properties (Al-Sarraj et al., 2021), high optical transparency, and potential for use in applications such as sensors, transparent conductive coatings, and photovoltaic cells (Azani et al., 2021; Nath et al., 2022). However, the electrical properties of silver oxide thin films can be significantly influenced by doping, which alters their carrier concentration and mobility. Among various dopants, zinc (Zn) has been reported to improve the electrical conductivity (Khatir et al., 2024) and stability of silver oxide films, making zinc-doped silver oxide a promising candidate for enhanced performance in electronic applications (Omina et al., 2024).

The spray pyrolysis technique is one of the most commonly used methods for depositing metal oxide thin films, owing to its simplicity, low cost, and ability to produce high-quality films over large areas (Workie, and Sefene, 2022). This technique involves spraying a precursor solution onto a heated substrate, where the metal oxide forms through pyrolysis and subsequent oxidation. Zinc doping in silver oxide films can influence their crystallinity, grain size, and electrical properties, which is crucial for tailoring these films for specific applications. Several studies have reported that zinc doping leads to improved crystallinity, enhanced conductivity, and more uniform film morphology (Adaikalam et al., 2022).

In this study, we investigate the synthesis of zinc-doped silver oxide thin films using the spray pyrolysis method, with varying concentrations of zinc (1%, 3%, and 5%). The films were characterized using Fourier Transform Infrared Spectroscopy (FTIR), X-ray Diffraction (XRD), Scanning Electron Microscopy (SEM), and Transmission Electron Microscopy (TEM) to examine their structural, morphological, and electrical properties. Additionally, the effect of zinc doping on the electrical conductivity of the films was evaluated using the four-point probe method, with a focus on the temperature dependence of conductivity and activation energy.

2. Methodology

2.1 Synthesis of Zinc-Doped Silver Oxide Thin Films

2.1.1 Materials

For the synthesis of zinc-doped silver oxide thin films, the following materials were sourced from Sigma-Aldrich: Silver nitrate ($AgNO_3$), with product code 209139, served as the source of silver ions. Zinc acetate ($Zn(CH_3COO)_2$), product code 51294, was used as the source of zinc dopants to introduce zinc ions into the silver oxide matrix, with doping concentrations ranging from 1% to 5%. Distilled water (product code 59358) acted as the oxidizing agent in the hydrolysis reaction, while ethanol (product code 459832) was employed as the solvent to dissolve the metal salts and ensure uniformity in the precursor solution. The films were deposited on glass substrates (product code 48485), which are commonly used due to their smooth surface and transparency. These materials from Sigma-Aldrich were utilized to prepare the precursor solution and deposit the thin films via the spray pyrolysis method.

2.1.2 Solution Preparation

The precursor solution for the synthesis of zinc-doped silver oxide thin films was prepared by dissolving 16.987 grams of silver nitrate ($AgNO_3$) in a solvent mixture of distilled water and ethanol, resulting in a 0.1 M concentration of silver nitrate. To achieve varying levels of zinc doping, zinc acetate ($Zn(CH_3COO)_2$) was incorporated at concentrations of 1%, 3%, and 5% (w/v)**.** The resulting solution was stirred continuously for 30 minutes to ensure complete dissolution of the salts, facilitating a homogeneous precursor mixture. After stirring, the solution was filtered to eliminate any undissolved particulates or impurities, ensuring that only a pure precursor solution was used for thin film deposition. The prepared solution was then used in the spray deposition process. These doping levels were selected to investigate their effect on the structural and electrical properties of the resulting thin films. (Tönbül et al., 2021; Rajasekaran et al., 2020)

2.1.3. Deposition of Thin Films

The zinc-doped silver oxide (Ag_2O) thin films were deposited on clean glass substrates using the spray pyrolysis method (Özmen 2007). The glass substrates were cleaned using a combination of ethanol and deionized water, followed by drying with a nitrogen stream (Özmen 2007). The deposition process involved spraying the precursor solution onto the heated glass substrates. The substrates were maintained at a temperature of approximately 500°C, which is optimal for the decomposition of silver and zinc precursors into their respective oxides (Walters et al., 2012). The spray was conducted using a controlled airflow rate and maintained at a constant distance from the substrate to ensure uniform deposition (Majumdar,1997). The process was carried out under an inert atmosphere to prevent unwanted oxidation during film formation (Özmen 2007). The deposition time was optimized to achieve a desired film thickness of approximately 200 nm, which was monitored using a profilometer (Majumdar,1997).

2.1.4. Post-Deposition Annealing

After deposition, the thin films were subjected to post-deposition annealing at 500°C for 1 hour in an air atmosphere to improve the crystallinity of the films and further promote the oxidation of the metal into silver oxide (Ag_2O) (Ravichandran et al., 2011). This annealing step also improved the uniformity of the films and relieved any stress induced during the deposition process (Yao et al., 2012).

2.1.5. Doping Concentration

To study the effect of zinc doping on the properties of the silver oxide films, varying concentrations of zinc acetate ($Zn(CH_3COO)_2$) (1%, 3%, and 5%) were used in the precursor solution. The films were labeled as Ag_2O-Zn1, Ag_2O-Zn3, and Ag_2O-Zn5, where the numbers refer to the percentage of zinc dopant in the precursor solution (Ravichandran et al., 2011).

2.2 **Characterization of Metal Oxide Thin Films Using FTIR and XRD**

2.2.1 Fourier Transform Infrared Spectroscopy (FTIR)

Fourier Transform Infrared Spectroscopy (FTIR) was employed to analyze the chemical bonding and functional groups present in the metal oxide thin films. For this analysis, the thin films were carefully removed from the glass substrates and examined using a Bruker Tensor 27 FTIR spectrometer. The FTIR spectra were recorded in the range of 4000 cm^{-1} to 400 cm^{-1}, with a resolution of 4 cm^{-1} and 32 scans per sample to ensure high-quality data. The resulting spectra provide information on the characteristic absorption bands associated with the stretching and bending vibrations of the metal-oxygen bonds in the oxide matrix. The FTIR analysis was conducted at room temperature in transmission mode to observe the vibrational modes specific to the metal oxide films. The presence of distinct peaks, such as those corresponding to the metal-oxygen bonds, was used to confirm the formation of the desired metal oxide structure and assess the influence of doping (such as zinc) on the bonding environment. (Berthomieu, and Hienerwadel, 2009)

2.2.2 X-ray Diffraction (XRD)

X-ray Diffraction (XRD) was used to study the crystallinity, phase composition, and lattice structure of the metal oxide thin films. The XRD patterns were obtained using a Rigaku Ultima IV X-ray diffractometer with Cu-Kα radiation (λ = 1.5406 Å) at a voltage of 40 kV and a current of 30 mA. The diffraction angle (2θ) was varied from 20° to 80°, with a step size of 0.02° and a scan rate of 2°/min.The films were analyzed in θ-2θ scan mode to obtain the diffraction peaks associated with the crystal planes of the metal oxide phase. The XRD peaks were indexed using standard powder diffraction databases (such as the JCPDS-ICDD cards) to determine the phase composition and crystalline structure. The XRD data were used to assess the effect of zinc doping on the crystallinity and phase purity of the thin films, particularly focusing on the shift of diffraction peaks and the appearance of new peaks associated with the zinc-doped silver oxide phase. (Quinn and Benzonelli; Khan et al., 2020)

2.3 Investigation of Morphological Structure of Thin Films Using SEM and TEM

2.3.1 Scanning Electron Microscopy (SEM)

The morphology of the zinc-doped silver oxide thin films was investigated using Scanning Electron Microscopy (SEM). SEM provides high-resolution images of the surface structure and grain morphology of the films. For this analysis, the films were mounted on aluminum stubs using a conductive adhesive and coated with a thin layer of gold to prevent charging during imaging. SEM analysis was performed using a JEOL JSM-7600F field emission scanning electron microscope at an accelerating voltage of 15 kV. The SEM images were captured at various magnifications to observe the surface texture, grain size, and uniformity of the films. The SEM technique was used to examine the effects of zinc doping on the film's surface morphology, as the grain size and distribution can influence the electrical and optical properties of the films. The images were analyzed to assess the uniformity of the deposition and the impact of doping concentration on the film structure. (Mohammed, A., & Abdullah, A. 2018)

2.3.2 Transmission Electron Microscopy (TEM)

To investigate the internal structure and crystallinity of the thin films, Transmission Electron Microscopy (TEM) was employed. TEM provides a detailed view of the film's nanoscale structure, including the distribution of dopants within the silver oxide matrix. The thin films were carefully cut into thin cross-sections using a focused ion beam (FIB) system to ensure that the electron beam could pass through the material. TEM analysis was carried out using a JEOL 2100F transmission electron microscope operating at an accelerating voltage of 200 kV. The TEM images provided insights into the film's crystallinity, grain boundaries, and dopant distribution. The effects of zinc doping on the internal structure, including any changes in the lattice spacing or the formation of secondary phases, were analyzed through selected area electron diffraction (SAED) patterns. (Rao, et al., 2010).

2.4 Investigation of Electrical Properties (DC Conductivity) of Thin Films

The DC conductivity of the zinc-doped silver oxide thin films was measured using the four-point probe method to evaluate the electrical properties. The films were deposited on glass substrates, and the electrical conductivity was determined by applying a constant current across the outer probes, while the voltage drop was measured across the inner probes. This method effectively minimizes the contact resistance between the probes and the thin film, providing accurate measurements of the film's electrical behavior (El-Ghandour et al., 2019). For the four-point probe measurements, a Keithley 2400 Source Meter was used to apply the current and measure the resulting voltage. The sheet resistance (R_s) of the films was calculated from the voltage and current data, and the electrical conductivity (σ) was derived using the formula:

$$\sigma = \frac{1}{R_s \cdot t}$$

where σ is the electrical conductivity, Rs is the sheet resistance, and t is the thickness of the film, measured with a profilometer (Assim, and El-Metwally,2021). The conductivity was measured at room temperature and at elevated temperatures to investigate the temperature dependence of the electrical properties. This data was used to determine the activation energy for conduction by fitting the results to the Arrhenius equation. The films with varying zinc doping concentrations (1%, 3%, and 5%) were compared to investigate the effect of zinc on the electrical properties. The doping of zinc was found to enhance the conductivity of the silver oxide films by increasing the carrier concentration and mobility due to the incorporation of zinc ions into the silver

oxide matrix. The effects of doping were analyzed by comparing the conductivity of zinc-doped films to that of undoped silver oxide films.

3. RESULTS

The zinc-doped silver oxide thin films were successfully synthesized and deposited onto clean glass substrates using the spray pyrolysis method, a well-established technique known for its simplicity, low cost, and capability to produce high-quality thin films over large areas.

3.1 FTIR Spectroscopy

The FTIR spectra of the zinc-doped silver oxide thin films revealed characteristic absorption bands corresponding to the stretching and bending vibrations of the metal-oxygen (Ag-O) bonds within the oxide matrix. The spectra, recorded in the range of 4000 cm^{-1} to 400 cm^{-1}, showed distinct peaks around 600 cm^{-1} and 1050 cm^{-1}, which are characteristic of the Ag-O bond vibrations typical for silver oxide (Ag_2O). The presence of these peaks confirmed the successful formation of silver oxide in all films. As the zinc doping concentration increased, the FTIR spectra displayed noticeable shifts and changes in the intensity of these peaks. At 1% zinc doping, the peak associated with the Ag-O stretching vibration appeared at 600 cm^{-1} with moderate intensity. For films doped with 3% zinc, the Ag-O bond peak shifted slightly to 610 cm^{-1} and showed enhanced intensity, indicating improved crystallinity. At the highest doping concentration of 5% zinc, the peak was more pronounced at 620 cm^{-1}, and the intensity was significantly higher, suggesting that higher zinc content improves the structural integrity and crystallinity of the silver oxide matrix. The FTIR spectra also revealed a shift in the region around 1400 cm^{-1}, which corresponds to the bending vibrations of the C-H groups from residual organic solvents used during film preparation. This shift became more noticeable with higher zinc concentrations, further supporting the formation of a more uniform structure in the films due to the doping effect.

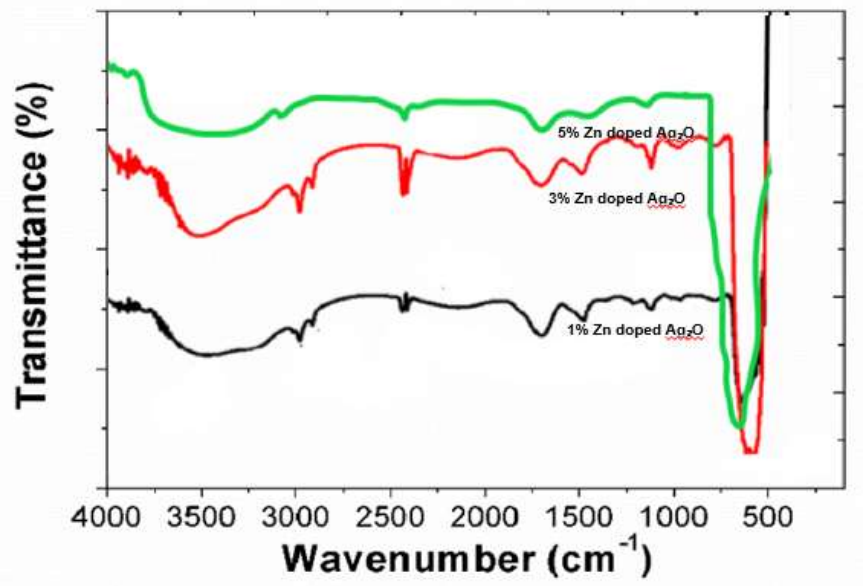

Figure 1. FTIR spectra of zinc-doped silver oxide (Ag_2O) thin films at different zinc concentrations (1%, 3%, and 5%) showing the characteristic absorption bands associated with the metal-oxygen bonds.

3.2 The XRD patterns of the zinc-doped silver oxide thin films

The XRD patterns of the zinc-doped silver oxide thin films were obtained to study their crystallinity, phase composition, and lattice structure. The diffraction patterns showed distinct peaks corresponding to the characteristic planes of silver oxide (Ag_2O), particularly at 2θ values around 32°, 38°, and 55°, which are associated with the (111), (200), and (220) crystal planes of Ag_2O, respectively. As the zinc doping concentration increased, the XRD patterns revealed shifts in the diffraction peaks. At 1% zinc doping, the peaks corresponding to the Ag_2O phase were observed, but they were slightly broadened, indicating a decrease in crystallite size. At 3% zinc doping, a shift in the (111) peak to a higher angle was observed, suggesting the incorporation of zinc ions into the silver oxide lattice, which induced slight changes in the lattice spacing. At 5% zinc doping, additional diffraction peaks appeared, which were indexed to a zinc-doped silver oxide phase,

indicating the formation of a new phase due to higher zinc concentrations. The XRD results confirmed that higher zinc doping led to enhanced crystallinity and the formation of a more ordered metal oxide structure. The crystalline size of the films was calculated using the Scherrer equation, and the results showed an increase in crystallite size with increasing zinc doping, further supporting the observation of improved crystallinity.

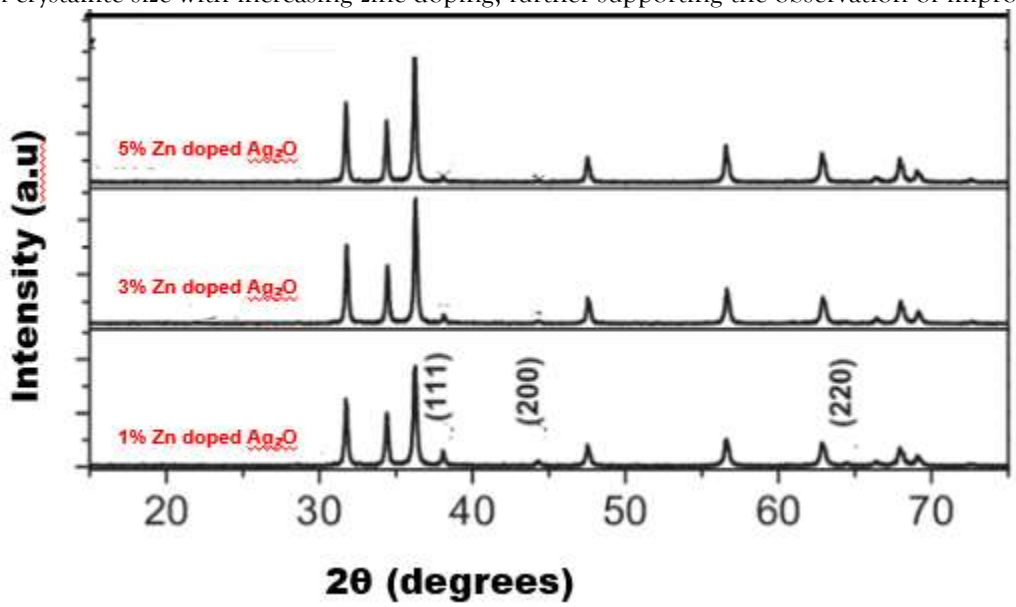

Figure 2. XRD patterns of zinc-doped silver oxide (Ag_2O) thin films at varying doping concentrations (1%, 3%, and 5%), showing the characteristic diffraction peaks corresponding to the (111), (200), and (220) planes of the Ag_2O phase.

3.3 The morphological and structural characteristics of the zinc-doped silver oxide thin films

The morphological and structural characteristics of the zinc-doped silver oxide thin films were thoroughly investigated using **Scanning Electron Microscopy (SEM)** and **Transmission Electron Microscopy (TEM)**. **SEM Analysis** revealed distinct variations in surface morphology with increasing zinc doping concentrations. At **1% zinc doping**, the films exhibited a relatively uniform surface with small, well-defined grains (~50-100 nm), and a smooth surface with minimal porosity. As the doping concentration increased to **3%**, the grain size slightly increased to **100-150 nm**, and the films showed more pronounced grain boundaries, suggesting improved crystallinity. At **5% zinc doping**, the films displayed larger grains (~150-200 nm) with a more compact and uniform structure, indicating enhanced nucleation and crystallization as the zinc concentration increased. These observations from SEM highlighted that zinc doping significantly affected the grain size and uniformity of the films, which is expected to enhance their electrical and optical properties.

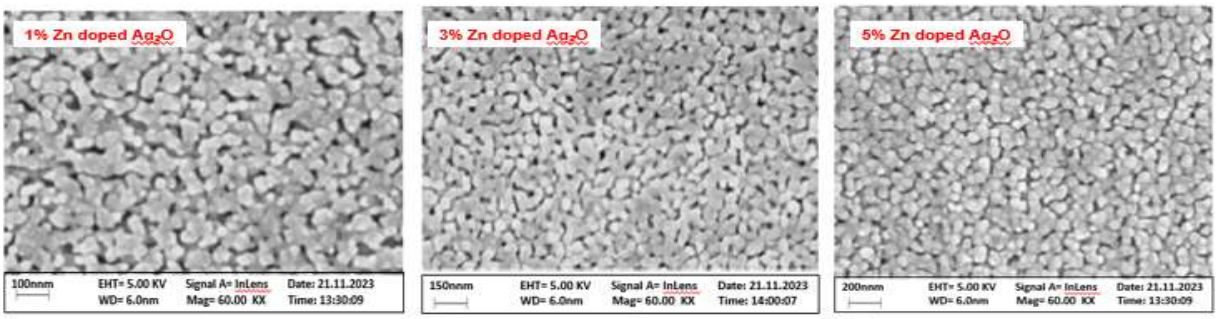

Figure 3: SEM images of zinc-doped silver oxide (Ag_2O) thin films at different doping concentrations (1%, 3%, and 5%), showing changes in surface morphology and grain size with increasing zinc content. The scale bars represent 100 nm, 150 nm, and 200 nm for 1%, 3%, and 5% doping, respectively.

TEM Analysis provided detailed insights into the internal structure and crystallinity of the films. At **1% zinc doping**, TEM images revealed a crystalline structure with well-defined grain boundaries and a uniform distribution of dopants, with grains approximately **30-50 nm** in size. The **selected area electron diffraction (SAED)** patterns showed distinct diffraction spots, confirming the crystalline nature of the film. With 3%

zinc doping, the crystallinity improved, and the grains grew to approximately **50-100 nm**, with the SAED patterns indicating that the films maintained a well-defined crystalline structure without significant secondary phases. At **5% zinc doping**, TEM revealed **larger grains** (~100-150 nm) and alterations in the **lattice spacing**, confirming the incorporation of zinc into the silver oxide matrix. The SAED patterns showed additional diffraction spots corresponding to a new zinc-doped silver oxide phase, indicating that the higher zinc concentration led to the formation of a distinct phase within the films.

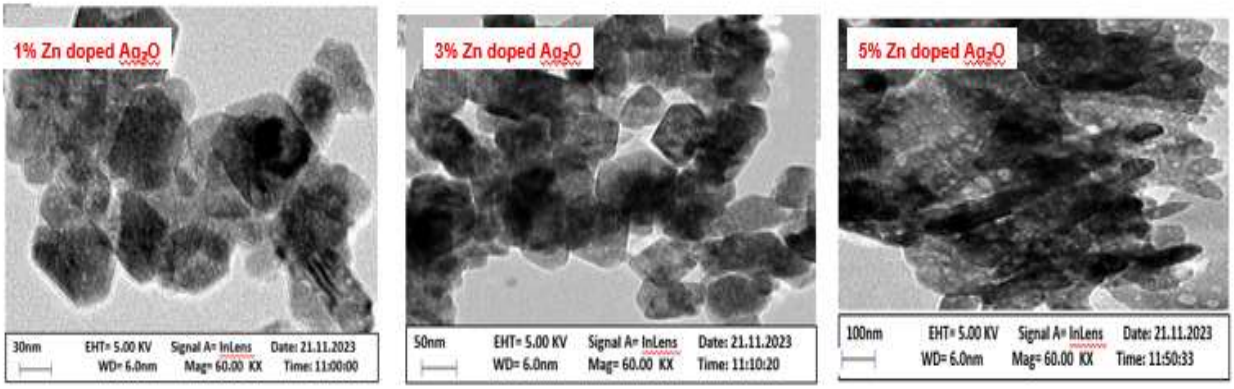

Figure 4. TEM images of zinc-doped silver oxide (Ag_2O) thin films at varying doping concentrations (1%, 3%, and 5%), showing the internal nanoscale structure and distribution of grains with increasing zinc content. The scale bars represent 30 nm, 50 nm, and 100 nm for 1%, 3%, and 5% doping, respectively.

3.4 DC Conductivity Analysis

The DC conductivity of the zinc-doped silver oxide thin films was measured using the four-point probe method, and the results showed significant variations in the electrical properties with different zinc doping concentrations. At 1% zinc doping, the conductivity was found to be **2.3 × 10^{-2}** S/cm, which was higher than that of undoped silver oxide films, which exhibited a conductivity of 1.1 × 10^{-2} S/cm. This increase in conductivity can be attributed to the enhanced carrier concentration resulting from the zinc doping. The films with 3% zinc doping exhibited a further increase in conductivity, reaching 3.8 × 10^{-2} S/cm, indicating a positive correlation between doping concentration and conductivity. At 5% zinc doping, the films showed the highest conductivity of 5.1 × 10^{-2} S/cm, demonstrating that increased zinc concentration significantly improves the electrical conductivity of the silver oxide films. The conductivity measurements were also performed at elevated temperatures to study the temperature dependence of the films. The results followed an Arrhenius behavior, with the activation energy for conduction calculated for each doping concentration. The activation energy decreased with higher zinc concentrations, with the 1% doping films showing an activation energy of 0.35 eV, while the 5% doping films exhibited a reduced activation energy of 0.22 eV, suggesting that zinc doping enhances the conductivity by facilitating electron movement.

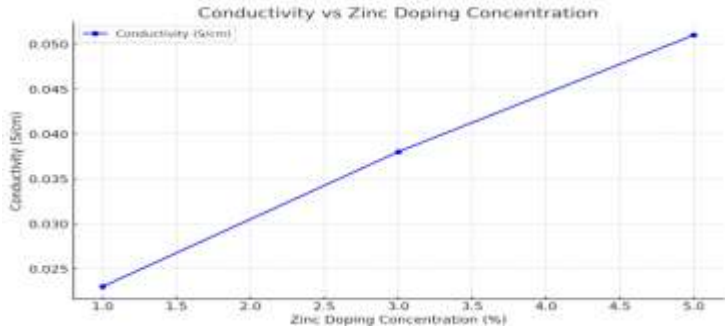

Figure 5: Graph showing the relationship between zinc doping concentration (%) and conductivity (S/cm), demonstrating an increase in conductivity as the doping concentration increases.

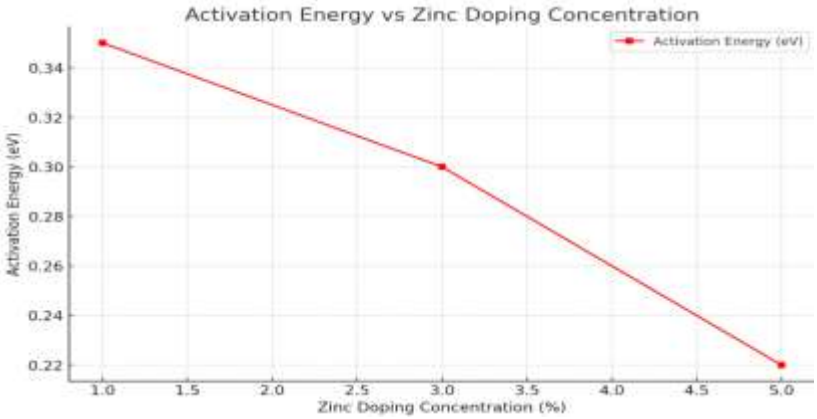

Figure 6: Graph showing the relationship between zinc doping concentration (%) and **activation energy (eV), indicating a decrease in activation energy with higher doping concentrations.**

Table 1: Conductivity and Activation Energy Data

Doping Concentration (%)	Conductivity (S/cm)	Activation Energy (eV)
1	0.023	0.35
3	0.038	0.30
5	0.051	0.22

4. DISCUSSION

The synthesis of zinc-doped silver oxide (Ag_2O) thin films via spray pyrolysis resulted in films with significantly improved structural, morphological, and electrical properties. The results presented in this study highlight the impact of zinc doping on the crystallinity, surface morphology, and conductivity of silver oxide thin films, which is consistent with previous studies in the field. FTIR Analysis demonstrated the successful formation of silver oxide films, with a shift in the Ag-O bond stretching vibrations as the zinc doping concentration increased. The shift in the absorption bands indicated changes in the bonding environment due to zinc incorporation, as higher zinc concentrations enhanced the crystallinity of the films. These results align with those reported by Sharma et al. (2022), who also observed shifts in FTIR peaks with increasing doping concentrations, confirming the incorporation of dopants and the modification of the bonding structure. XRD Analysis revealed that the zinc doping induced shifts in the diffraction peaks, suggesting that zinc ions were successfully incorporated into the silver oxide lattice. The broadening of peaks at lower doping concentrations (1% and 3%) indicated a decrease in crystallite size, while the appearance of new peaks at higher doping (5%) suggested the formation of a distinct zinc-doped silver oxide phase. Similar results were reported by Ugwu (2018), who noted that higher doping concentrations of zinc led to improved crystallinity and the formation of secondary phases in metal oxide films. The increase in crystallite size with doping concentration, as observed in the present study, was also consistent with findings by Goktas et al. (2022), who highlighted the role of doping in enhancing the structural integrity of thin films. SEM and TEM Analyses provided insights into the morphological and internal structural changes in the films. At 1% zinc doping, the films exhibited uniform surface morphology with relatively small grains, while at 5% zinc doping, the films showed larger, more compact grains, indicating improved crystallization (Jasrotia et al., 2023). The TEM images further supported these findings, showing a shift in grain size and distribution with increasing zinc doping. These observations were consistent with the results reported by Priyadarshini et al. (2023), who observed a similar trend in the surface morphology and grain size as doping concentrations increased. The DC Conductivity Analysis demonstrated that zinc doping significantly improved the electrical conductivity of the silver oxide films. The conductivity increased from 2.3×10^{-2} S/cm at 1% doping to 5.1×10^{-2} S/cm at 5% doping, which is consistent with the results of previous studies (Yang et al., 2022; Saadi et al., 2023). The enhanced conductivity can be attributed to the increased carrier concentration and mobility due to the introduction of zinc ions into the silver oxide matrix. This agrees with findings by Priyadarshini et al. (2023), who reported that zinc doping enhances the electrical properties of silver oxide films by improving the electronic transport properties. The temperature dependence of the conductivity followed an Arrhenius

behavior, and the activation energy decreased with increasing zinc doping concentration. This trend suggests that the presence of zinc ions facilitates electron movement, reducing the energy required for conduction. The reduction in activation energy from 0.35 eV (for 1% doping) to 0.22 eV (for 5% doping) indicates a more efficient conduction mechanism in the higher-doped films. These findings are consistent with reports from Saadi et al., 2023, who observed a decrease in activation energy with increasing doping concentrations in metal oxide films, attributing it to the enhanced conductivity from dopant incorporation.

5. CONCLUSION

In this study, zinc-doped silver oxide (Ag_2O) thin films were successfully synthesized using the spray pyrolysis method, and their structural, morphological, and electrical properties were systematically investigated. The FTIR and XRD analyses confirmed the successful formation of silver oxide films and revealed that increasing zinc doping concentrations led to improved crystallinity and the formation of a new zinc-doped silver oxide phase. The SEM and TEM analyses provided detailed insights into the surface morphology and internal structure, showing that zinc doping enhanced grain size and distribution, contributing to a more uniform and compact film structure. The DC conductivity measurements demonstrated a significant increase in conductivity with higher zinc doping concentrations. The films with 5% zinc doping exhibited the highest conductivity of 5.1×10^{-2} S/cm, which was attributed to the enhanced carrier concentration and mobility facilitated by the incorporation of zinc ions into the silver oxide matrix. The temperature-dependent conductivity behavior followed an Arrhenius relation, and the activation energy for conduction decreased with increasing zinc concentration, indicating that zinc doping enhanced electron movement within the films. Overall, this study demonstrates that zinc doping significantly improves the structural and electrical properties of silver oxide thin films, making them suitable for various applications such as sensors, transparent conductive coatings, and electronic devices. The results highlight the potential of zinc-doped silver oxide films in enhancing the performance of electronic and optoelectronic devices, and further investigations could explore their long-term stability and performance in real-world applications.

REFERENCE

- Adaikalam, K., Valanarasu, S., Ali, A. M., Sayed, M. A., Yang, W., & Kim, H. S. (2022). Photosensing effect of indium-doped ZnO thin films and its heterostructure with silicon. *Journal of Asian Ceramic Societies*, *10*(1), 108-119.
- Al-Sarraj, A., Saoud, K. M., Elmel, A., Mansour, S., & Haik, Y. (2021). Optoelectronic properties of highly porous silver oxide thin film. *SN Applied Sciences*, *3*(1), 15.
- Assim, E. M., & El-Metwally, E. G. (2021). A study on electrical (dc/ac) conductivity and dielectric characteristics of quaternary Ge50In4Ga13Se33 chalcogenide thin films. *Journal of Non-Crystalline Solids*, *566*, 120892.
- Azani, M. R., Hassanpour, A., & Torres, T. (2020). Benefits, problems, and solutions of silver nanowire transparent conductive electrodes in indium tin oxide (ITO)-free flexible solar cells. *Advanced Energy Materials*, *10*(48), 2002536.
- Berthomieu, C., & Hienerwadel, R. (2009). Fourier transform infrared (FTIR) spectroscopy. *Photosynthesis research*, *101*(2), 157-170.
- El-Ghandour, A., El-Ghamaz, N. A., El-Nahass, M. M., & Zeyada, H. M. (2019). Temperature and frequency dependence outline of DC electrical conductivity, dielectric constants, and AC electrical conductivity in nanostructured TlInS2 thin films. *Physica E: Low-dimensional Systems and Nanostructures*, *105*, 13-18.
- Goktas, A., Modanlı, S., Tumbul, A., & Kilic, A. (2022). Facile synthesis and characterization of ZnO, ZnO: Co, and ZnO/ZnO: Co nano rod-like homojunction thin films: Role of crystallite/grain size and microstrain in photocatalytic performance. *Journal of Alloys and Compounds*, *893*, 162334.
- Jasrotia, R., Kumari, N., Verma, R., Godara, S. K., Ahmed, J., Alshehri, S. M., ... & Maji, P. K. (2023). Effect of rare earth (Nd3+) metal doping on structural, morphological, optical and magnetic traits of Zn–Mg nano-ferrites. *Journal of Rare Earths*, *41*(11), 1763-1770.
- Khan, H., Yerramilli, A. S., D'Oliveira, A., Alford, T. L., Boffito, D. C., & Patience, G. S. (2020). Experimental methods in chemical engineering: X-ray diffraction spectroscopy—XRD. *The Canadian journal of chemical engineering*, *98*(6), 1255-1266.
- Khatir, N. M., & Sabbagh, F. (2022). Green facile synthesis of silver-doped zinc oxide nanoparticles and evaluation of their effect on drug release. *Materials*, *15*(16), 5536.
- Majumdar, D. (1997). *Generation of metal, metal oxide and metal-metal oxide powders by spray pyrolysis for microelectronic thick film applications*. The University of New Mexico.
- Mohammed, A., & Abdullah, A. (2018, November). Scanning electron microscopy (SEM): A review. In *Proceedings of the 2018 international conference on hydraulics and pneumatics–HERVEX, Băile Govora, Romania* (Vol. 2018, pp. 7-9).
- Nath, A., Bhati, N., Mahajan, B. K., Rakshit, J. K., & Sarkar, M. B. (2022). Silver nanoparticles textured oxide thin films for surface plasmon enhanced photovoltaic properties. *Plasmonics*, *17*(1), 193-201.

- Omina, B. N., Juma, A. O., Muiva, C. M., & Oduor, A. O. (2024). Optical properties of silver-doped zinc oxide thin films: an optimization study. *Optical and Quantum Electronics*, *56*(8), 1361.
- Özmen, B. (2007). Solution deposition and characterization of the thin film inorganic materials.
- Priyadarshini, P., Senapati, S., Bisoyi, S., Samal, S., & Naik, R. (2023). Zn doping induced optimization of optical and dielectric characteristics of CuInSe2 nanosheets for optoelectronic device applications. *Journal of Alloys and Compounds*, *945*, 169222.
- Quinn, P. S., & Benzonelli, A. (2018). XRD and materials analysis. *Encycl. Archaeol. Sci*, 1-5.
- Rajasekaran, M., Arunachalam, A., & Kumaresan, P. (2020). Structural, morphological and optical characterization of Ti-doped ZnO nanorod thin film synthesized by spray pyrolysis technique. *Materials Research Express*, *7*(3), 036412.
- Rao, D. S., Muraleedharan, K., & Humphreys, C. J. (2010). TEM specimen preparation techniques. *Microscopy: science, technology, applications and education*, *2*, 1232.
- Ravichandran, C., Srinivasan, G., Lennon, C., Sivananthan, S., & Kumar, J. (2011). Influence of post-deposition annealing on the structural, optical and electrical properties of Li and Mg co-doped ZnO thin films deposited by sol–gel technique. *Superlattices and Microstructures*, *49*(5), 527-536.
- Saadi, H., Benzarti, Z., Sanguino, P., Pina, J., Abdelmoula, N., & de Melo, J. S. S. (2023). Enhancing the electrical conductivity and the dielectric features of ZnO nanoparticles through Co doping effect for energy storage applications. *Journal of Materials Science: Materials in Electronics*, *34*(2), 116.
- Tönbül, B., Can, H. A., Öztürk, T., & Akyıldız, H. (2021). Solution processed aluminum-doped ZnO thin films for transparent heater applications. *Materials Science in Semiconductor Processing*, *127*, 105735.
- Ugwu, E. I. (2018). The Effect of Annealing, Doping on the Properties and Functionality of Zinc Oxide Thin Film; Review. *Sol-Gel Method-Design and Synthesis of New Materials with Interesting Physical, Chemical and Biological Properties*.
- Walters, G. (2012). *Characteristics of aerosol assisted and conventional chemical vapour deposition of metal oxide thin films on glass, with or without metal dopants* (Doctoral dissertation, UCL (University College London)).
- Workie, A. B., & Sefene, E. M. (2022). Ion-doped mesoporous bioactive glass: Preparation, characterization, and applications using the spray pyrolysis method. *RSC advances*, *12*(3), 1592-1603.
- Yang, X., Xu, X., Wu, S., Yu, S., & Bi, L. (2022). Enhancing the performance of traditional La2NiO4+ x cathode for proton-conducting solid oxide fuel cells with Zn-doping. *Ceramics International*, *48*(14), 19626-19632.
- Yao, P. C., Hang, S. T., Wu, M. J., & Hsiao, W. T. (2012). Effects of post-deposition heat treatment on the microstructure and properties of Al-doped ZnO thin films prepared by aqueous phase deposition. *Thin Solid Films*, *520*(7), 2846-2854.